

# A Front-Tracking Method for Motion by Mean Curvature with Surfactant

Ming-Chih Lai\*   Che-Wei Hsu<sup>†</sup>   Huaxiong Huang<sup>‡</sup>

## Abstract

In this paper, we present a finite difference method to track a network of curves whose motion is determined by mean curvature. To study the effect of inhomogeneous surface tension on the evolution of the network of curves, we include surfactant which can diffuse along the curves. The governing equations consist of one parabolic equation for the curve motion coupled with a convection-diffusion equation for the surfactant concentration along each curve. Our numerical method is based on a direct discretization of the governing equations which conserves the total surfactant mass in the curve network. Numerical experiments are carried out to examine the effects of inhomogeneous surface tension on the motion of the network, including the von Neumann law for cell growth in two space dimensions.

Keywords: Front-tracking method; Motion by mean curvature; Triple-junction; Surface tension; Surfactant

## 1 Problem Description

Interface phenomena have been studied extensively not only due to their importance in applications but also for the computational challenges they

---

\*Corresponding author. Department of Applied Mathematics, National Chiao Tung University, 1001, Ta Hsueh Road, Hsinchu 300, Taiwan. E-mail: mclai@math.nctu.edu.tw

<sup>†</sup>Department of Applied Mathematics, National Chiao Tung University, 1001, Ta Hsueh Road, Hsinchu 300, Taiwan.

<sup>‡</sup>Department of Mathematics and Statistics, York University, Toronto, Ontario, Canada M3J 1P3. Email: hhuang@yorku.ca

impose. Motion by mean curvature has been used as a model for various physical problems including multiphase flows and growth of grain boundary in poly-crystals [3]. Level-set method is a popular choice for these type of problems [9]. In [1], a direct finite difference method was used to study the evolution of a network of curves due to its simplicity and efficiency.

In this paper, we generalize the grain growth problem discussed in [1] by including the effect of an inhomogeneous surface tension. For practical problems, it is difficult to maintain constant surface tension as insoluble surface active agents (surfactant) are common and their presence could significantly affect the value of the surface tension, therefore the dynamics of interface motion [2]. To account for the effect of the surface tension on the interfacial dynamics of a complex network of interfaces, we consider a network of curves in a two dimensional setting and assume that there is a surfactant distributed along the curve and the surface tension varies according to the surfactant concentration. As in [1], we consider the situation with triple-junctions, i.e., three phase boundaries, described by parametric curves  $\mathbf{X}^i(s, t)$ ,  $s \in [0, 1]$  for  $i = 1, 2, 3$  as shown in Fig. 1. Throughout this paper, we define  $\boldsymbol{\tau}^i(s, t) = \mathbf{X}_s^i/|\mathbf{X}_s^i|$  as the unit tangent vector of the curve  $i$ . The motion of equations are defined as

$$\mathbf{X}_t^i = \sigma^i \frac{\mathbf{X}_{ss}^i}{|\mathbf{X}_s^i|^2}, \quad (1)$$

where  $\sigma^i(s, t)$  is the surface tension along the curve  $\mathbf{X}^i$  and is determined by the surfactant concentration  $\Gamma^i(s, t)$ . By taking inner product with normal vector  $\mathbf{n}^i = \mathbf{X}_s^{i\perp}/|\mathbf{X}_s^i|$ , Eq. (1) becomes

$$\mathbf{X}_t^i \cdot \mathbf{n}^i = \sigma^i \frac{\mathbf{X}_{ss}^i}{|\mathbf{X}_s^i|^2} \cdot \frac{\mathbf{X}_s^{i\perp}}{|\mathbf{X}_s^i|} = \sigma^i \kappa^i, \quad (2)$$

where  $\kappa^i$  is the local mean curvature of the curve  $\mathbf{X}^i$ . Thus the normal velocity of curve motion is proportional to the local mean curvature and the surface tension coefficient.

The presence of surfactant reduces the surface tension, and in this paper we use the simplified nonlinear Langmuir equation of state [10]

$$\sigma^i = \sigma_c(1 + \ln(1 - \beta^i \Gamma^i)). \quad (3)$$

Along the curve, the surfactant concentration is governed by the transport equation [12, 4]

$$\Gamma_t^i + (\nabla_s \cdot \mathbf{U}^i) \Gamma^i = \mu \nabla_s^2 \Gamma^i, \quad (4)$$

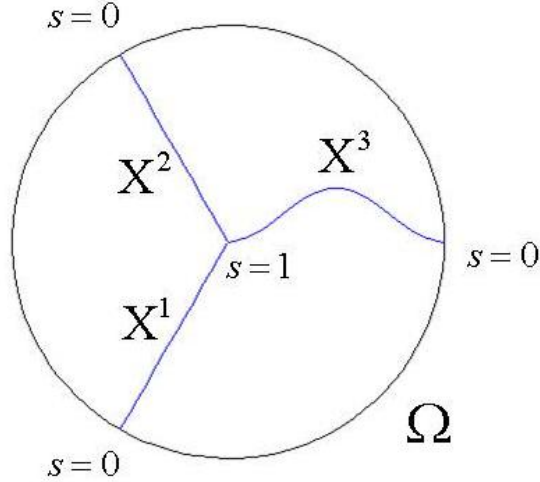


Fig. 1: A three-curve network.

where  $\nabla_s$  is the surface gradient operator and  $\nabla_s^2 = \nabla_s \cdot \nabla_s$  is the surface Laplacian.  $\mathbf{U}^i = \mathbf{X}_t^i$  is the velocity of the curve. In this paper, the diffusion coefficient of the surfactant concentration  $\mu$  is assumed to be a constant for all curves. Note that the above time derivative is taken by fixing the tracking parameter  $s$ . Therefore, our equation is different from the one derived by Stone [11] where the time derivative is taken with respect to the fixed Eulerian position. For clarity, the above surface divergence and surface Laplacian can be written explicitly as

$$\nabla_s \cdot \mathbf{U}^i = \frac{\partial \mathbf{U}^i}{\partial \boldsymbol{\tau}^i} \cdot \boldsymbol{\tau}^i = \frac{\partial \mathbf{U}^i}{\partial s} \cdot \boldsymbol{\tau}^i \left/ \left| \frac{\partial \mathbf{X}^i}{\partial s} \right| \right. \quad (5)$$

$$\nabla_s^2 \Gamma^i = \frac{\partial}{\partial s} \left( \frac{\partial \Gamma^i}{\partial s} \left/ \left| \frac{\partial \mathbf{X}^i}{\partial s} \right| \right) \right) \left/ \left| \frac{\partial \mathbf{X}^i}{\partial s} \right| \right. . \quad (6)$$

We assume that each curve meets the domain boundary with a right angle at  $s = 0$ . More precisely, let  $\mathbf{b}(\alpha)$  be the given parametric representation of the domain with  $\alpha \in [0, 2\pi]$ . The conditions at the domain boundary are given by

$$\mathbf{X}^i(0, t) = \mathbf{b}(\alpha_i) \quad (7)$$

for some  $\alpha_i$  such that

$$\boldsymbol{\tau}^i(0, t) \cdot \mathbf{b}'(\alpha_i) = 0. \quad (8)$$

We further assume that there is no surfactant flux across the domain boundary

$$\nabla_s \Gamma^i(0, t) \cdot \boldsymbol{\tau}^i(0, t) = \frac{\partial \Gamma^i}{\partial s}(0, t) = 0. \quad (9)$$

At the triple-junction ( $s = 1$ ), three curves meet and we have geometric constraints

$$\mathbf{X}^1(1, t) = \mathbf{X}^2(1, t) = \mathbf{X}^3(1, t). \quad (10)$$

Since the above conditions only provide two equations for three curves, one more condition is required, which comes from the Young-Laplace equation (balance of surface tension)

$$\sum_{i=1}^3 \sigma^i(1, t) \boldsymbol{\tau}^i(1, t) = 0 \quad (11)$$

where the tangent vectors join at and point away from the triple-junction. When  $\beta^i$  are identical, the surface tensions take the same value at the junction. Thus, the Young-Laplace condition implies that the angles between these curves are 120 degree which results in the famous law of Plateau.

We also need to impose the boundary conditions for surfactant concentration at the triple-junction

$$\Gamma^1(1, t) = \Gamma^2(1, t) = \Gamma^3(1, t) \quad (12)$$

$$\sum_{i=1}^3 \nabla_s \Gamma^i(1, t) \cdot \boldsymbol{\tau}^i(1, t) = \sum_{i=1}^3 \frac{\partial \Gamma^i}{\partial s}(1, t) \left/ \left| \frac{\partial \mathbf{X}^i}{\partial s}(1, t) \right| \right. = 0. \quad (13)$$

Eq. (12) represents the continuity of the surfactant concentration, while Eq. (13) implies zero net tangential flux at the triple-junction. From the surfactant equation (4) and boundary conditions Eq. (9)-(13), we can easily verify that the total surfactant mass along the three curves is conserved, i.e.,

$$\frac{d}{dt} \left( \sum_{i=1}^3 \int_0^1 \Gamma^i(s, t) \left| \frac{\partial \mathbf{X}^i}{\partial s} \right| ds \right) = 0. \quad (14)$$

## 2 Numerical Method

For each parametric curve  $i$ , we set up a mesh  $s_k = (k - 1/2)\Delta s, k = 1, 2, \dots, M$  where  $\Delta s = 1/M$ , and use a collection of discrete points (Lagrangian markers)  $\mathbf{X}_k^i = \mathbf{X}^i(s_k, n\Delta t)$  to represent the curve at time  $t = n\Delta t$ . The surfactant concentrations and surface tensions on each curve are also defined on these Lagrangian markers and denoted by  $\Gamma_k^i = \Gamma^i(s_k, n\Delta t)$  and  $\sigma_k^i = \sigma^i(s_k, n\Delta t)$ , respectively. For clarity, we use the variables with tilde as the values at the next time step; that is,  $\tilde{\mathbf{X}}_k^i = \mathbf{X}^i(s_k, (n+1)\Delta t)$  and  $\tilde{\Gamma}_k^i = \Gamma^i(s_k, (n+1)\Delta t)$ . The motion of the curves is computed by advancing the values  $\mathbf{X}_k^i, \Gamma_k^i$  at time step  $n\Delta t$  to  $\tilde{\mathbf{X}}_k^i, \tilde{\Gamma}_k^i$  at time step  $(n+1)\Delta t$ . The numerical time integration consists of the following steps.

1. Compute the surface tension on each curve  $i$

$$\sigma_k^i = \sigma_c(1 + \ln(1 - \beta^i \Gamma_k^i)), \quad k = 1, 2, \dots, M \quad (15)$$

2. Solve the equation of motion (1) by an explicit scheme as in [1]

$$\frac{\tilde{\mathbf{X}}_k^i - \mathbf{X}_k^i}{\Delta t} = \sigma_k^i \frac{(\mathbf{X}_{k+1}^i - 2\mathbf{X}_k^i + \mathbf{X}_{k-1}^i)/\Delta s^2}{|(\mathbf{X}_{k+1}^i - \mathbf{X}_{k-1}^i)/(2\Delta s)|^2}. \quad (16)$$

Here, we use the central difference schemes to approximate the first and second derivatives. Note that the above discretization is valid at the interior points  $k = 1, 2, \dots, M$ . Next we provide the details on how to find the boundary points  $\tilde{\mathbf{X}}_0^i$  and  $\tilde{\mathbf{X}}_{M+1}^i$  which are associated with the domain boundary  $s = 0$  and the triple-junction  $s = 1$ , respectively.

- (a) At the domain boundary, we discretize Eqs. (7) and (8) by central difference approximation as

$$\frac{\tilde{\mathbf{X}}_1^i + \tilde{\mathbf{X}}_0^i}{2} = \mathbf{b}(\alpha^i), \quad \frac{\tilde{\mathbf{X}}_1^i - \tilde{\mathbf{X}}_0^i}{\Delta s} \cdot \mathbf{b}'(\alpha^i) = 0, \quad (17)$$

from which we obtain

$$(\tilde{\mathbf{X}}_1^i - \mathbf{b}(\alpha^i)) \cdot \mathbf{b}'(\alpha^i) = 0. \quad (18)$$

Since the boundary curve  $\mathbf{b}(\alpha)$  and its tangent  $\mathbf{b}'(\alpha)$  is known analytically, the above scalar algebraic equation can be solved

very easily. Once  $\alpha^i$  is found, the domain boundary point can be extrapolated by

$$\tilde{\mathbf{X}}_0^i = 2\mathbf{b}(\alpha^i) - \tilde{\mathbf{X}}_1^i. \quad (19)$$

(b) At the triple-junction, we discretize Eqs. (10) and (11) as

$$\frac{\tilde{\mathbf{X}}_{M+1}^1 + \tilde{\mathbf{X}}_M^1}{2} = \frac{\tilde{\mathbf{X}}_{M+1}^2 + \tilde{\mathbf{X}}_M^2}{2} = \frac{\tilde{\mathbf{X}}_{M+1}^3 + \tilde{\mathbf{X}}_M^3}{2} = \tilde{\mathbf{X}}_p, \quad (20)$$

$$\sigma_p^1 \frac{\tilde{\mathbf{X}}_p - \tilde{\mathbf{X}}_M^1}{|\tilde{\mathbf{X}}_p - \tilde{\mathbf{X}}_M^1|} + \sigma_p^2 \frac{\tilde{\mathbf{X}}_p - \tilde{\mathbf{X}}_M^2}{|\tilde{\mathbf{X}}_p - \tilde{\mathbf{X}}_M^2|} + \sigma_p^3 \frac{\tilde{\mathbf{X}}_p - \tilde{\mathbf{X}}_M^3}{|\tilde{\mathbf{X}}_p - \tilde{\mathbf{X}}_M^3|} = 0. \quad (21)$$

The details of marker location at the triple-junction can be found in Fig. 2.

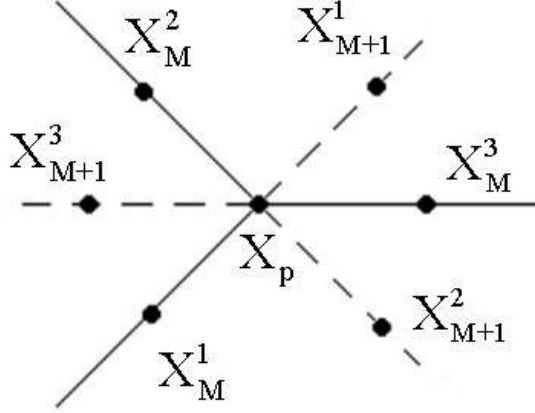


Fig. 2: Details of marker location at the triple-junction.

- Update surfactant concentration  $\tilde{\Gamma}_k^i$  as follows. Firstly, we rewrite the surfactant concentration in a form as

$$\frac{\partial \Gamma^i}{\partial t} \left| \frac{\partial \mathbf{X}^i}{\partial s} \right| + \frac{\partial}{\partial t} \left| \frac{\partial \mathbf{X}^i}{\partial s} \right| \Gamma^i = \mu \frac{\partial}{\partial s} \left( \frac{\partial \Gamma^i}{\partial s} \left/ \left| \frac{\partial \mathbf{X}^i}{\partial s} \right| \right. \right), \quad (22)$$

by multiplying (4) with the stretching factor  $\left| \frac{\partial \mathbf{X}^i}{\partial s} \right|$  and using the following equation [4]

$$\frac{\partial}{\partial t} \left| \frac{\partial \mathbf{X}^i}{\partial s} \right| = (\nabla_s \cdot \mathbf{U}^i) \left| \frac{\partial \mathbf{X}^i}{\partial s} \right|. \quad (23)$$

Denoting the discrete stretching factor by

$$|D_s \mathbf{X}_{k+1/2}^i| = \left| \frac{\mathbf{X}_{k+1}^i - \mathbf{X}_k^i}{\Delta s} \right|, \quad (24)$$

$$|D_s \mathbf{X}_k^i| = \frac{1}{2} (|D_s \mathbf{X}_{k+1/2}^i| + |D_s \mathbf{X}_{k-1/2}^i|), \quad (25)$$

we can now discretize (22) by an explicit and symmetric scheme as

$$\begin{aligned} & \frac{\tilde{\Gamma}_k^i - \Gamma_k^i}{\Delta t} \frac{|D_s \tilde{\mathbf{X}}_k^i| + |D_s \mathbf{X}_k^i|}{2} + \frac{|D_s \tilde{\mathbf{X}}_k^i| - |D_s \mathbf{X}_k^i|}{\Delta t} \frac{\tilde{\Gamma}_k^i + \Gamma_k^i}{2} \\ &= \mu \frac{1}{\Delta s} \left( \frac{(\Gamma_{k+1}^i - \Gamma_k^i)/\Delta s}{|D_s \mathbf{X}_{k+1/2}^i|} - \frac{(\Gamma_k^i - \Gamma_{k-1}^i)/\Delta s}{|D_s \mathbf{X}_{k-1/2}^i|} \right) \end{aligned} \quad (26)$$

on the interior points  $k = 1, 2 \dots M$ . For the values on the boundary points  $\tilde{\Gamma}_0^i$  and  $\tilde{\Gamma}_{M+1}^i$ , we will use the conditions at domain boundary  $s = 0$  and the triple-junction  $s = 1$ , respectively.

- (a) At the domain boundary  $s = 0$ , we use central difference to discretize Eq. (9) and obtain  $\tilde{\Gamma}_0^i = \tilde{\Gamma}_1^i$ .
- (b) At the triple-junction  $s = 1$ , we approximate Eqs. (12) and (13) by

$$\begin{aligned} & \frac{\tilde{\Gamma}_{M+1}^1 + \tilde{\Gamma}_M^1}{2} = \frac{\tilde{\Gamma}_{M+1}^2 + \tilde{\Gamma}_M^2}{2} = \frac{\tilde{\Gamma}_{M+1}^3 + \tilde{\Gamma}_M^3}{2} = \tilde{\Gamma}_p, \quad (27) \\ & \frac{(\tilde{\Gamma}_{M+1}^1 - \tilde{\Gamma}_M^1)/\Delta s}{|D_s \tilde{\mathbf{X}}_{M+1/2}^1|} + \frac{(\tilde{\Gamma}_{M+1}^2 - \tilde{\Gamma}_M^2)/\Delta s}{|D_s \tilde{\mathbf{X}}_{M+1/2}^2|} + \frac{(\tilde{\Gamma}_{M+1}^3 - \tilde{\Gamma}_M^3)/\Delta s}{|D_s \tilde{\mathbf{X}}_{M+1/2}^3|} \\ &= 0 \end{aligned} \quad (28)$$

Substituting Eq. (27) into Eq. (28) yields an single equation for surfactant concentration at the triple-junction  $\tilde{\Gamma}_p$ . Once  $\tilde{\Gamma}_p$  is found,  $\tilde{\Gamma}_{M+1}^i$  can be easily obtained from Eq. (27).

Note that, by taking the summation of both sides of Eq. (26) and using the numerical boundary condition at the triple-junction (28), one can easily verify that

$$\sum_{i=1}^3 \sum_{k=1}^M \tilde{\Gamma}_k^i |D_s \tilde{\mathbf{X}}_k^i| \Delta s = \sum_{i=1}^3 \sum_{k=1}^M \Gamma_k^i |D_s \mathbf{X}_k^i| \Delta s. \quad (29)$$

This is the discrete version of the conservation of total surfactant mass along all the curves, corresponding to the mid-point rule discretization for the integral in Eq. (14).

It is interesting to note that the numerical scheme (16) for Eq. (1) is independent of the mesh width  $\Delta s$ . Since the scheme is explicit, the time step size must be chosen similarly in [1] by

$$\Delta t = \frac{1}{8} \min_{\{i,k\}} \frac{|\mathbf{X}_{k+1}^i - \mathbf{X}_{k-1}^i|^2}{\sigma_k^i}. \quad (30)$$

Under this constraint, the time step becomes smaller if the length of any curve shortens in which the marker spacing becomes smaller. One way to maintain the marker resolution is to delete the markers in an appropriate way so that the time step size can be maintained. On the other hand, if the curve stretches and the marker spacing is too coarse, then we need to add more markers along the curve. The details of marker redistribution technique can be found in [1, 4]. One important thing during the marker redistribution process is to keep the mass conservation of the surfactant. This can be done in a local way. For instance, in the segment of adding more marker points, we simply distribute the surfactant mass into those points uniformly. On the other hand, in the segment of removing marker points, we add up those surfactant mass to be a new surfactant concentration in the new combining segment. Thus, the overall surfactant mass is conserved exactly without any scaling.

### 3 Numerical Results

As in [1], we consider the network of curves inside the unit disk such that  $\mathbf{b}(\alpha) = (\sin \alpha, \cos \alpha)$ , where  $\alpha \in [0, 2\pi]$ . For comparison purposes, we will present results for the cases without surfactant (clean) and with surfactant (contaminated). Using the equation of state given by Eq. (15),  $\beta^i=0$  implies no surfactant exists on the curves, in which we do not need to solve the surfactant equation (4). Thus, the clean network of curves has a uniform surface tension  $\sigma = \sigma_c = 1$ . For the following test, we choose the mesh width on each curve  $\Delta s = 1/16$  and the time step  $\Delta t = 0.0001$ .

### 3.1 Three-curve network

As the first example, we consider the evolution of three curves in the unit disk with initial configuration as in [1]

$$\mathbf{X}^1(s, 0) = (1 - s)(-1/2, -\sqrt{3}/2) \quad (31)$$

$$\mathbf{X}^2(s, 0) = (1 - s)(-1/2, \sqrt{3}/2) \quad (32)$$

$$\mathbf{X}^3(s, 0) = (1 - s, \sin^2(\pi s)/4). \quad (33)$$

The above initial configuration is shown in Fig. 1. To examine the effect of the surfactant on the curves motion, we compare the cases with ( $\beta^i = 0.25, i = 1, 2, 3$ ) and without surfactant ( $\beta^i=0, i = 1, 2, 3$ ). For the case with surfactant, the diffusion coefficient is chosen as  $\mu = 0.1$ . The initial surfactant concentration is uniformly distributed only along the curve 3 so that  $\Gamma^1(s, 0) = \Gamma^2(s, 0) = 0$  and  $\Gamma^3(s, 0) = 1$ .

Fig. 3 shows the time evolution of these three curve networks. We denote the clean curve network (without surfactant) by solid line, while the contaminated curve network (with surfactant) by dotted line. As demonstrated in [1], the curve 3 will be flattered out to make the shape between curves 2 and 3 convex. Thus, the area between between curves 2 and 3 decrease as time evolves. Since the existence of the surfactant along the curve 3 reduces the surface tension, the curve motion becomes slower than the clean curve network. Fig. 4 shows the surfactant distribution along each curves. One can easily see that due to the effect of diffusion, the surfactant on curves 1 and 2 are no longer zero.

### 3.2 von Neumann law

In 1952, von Neumann [7] showed that the rate of the change of the area of a given bubble (a curved polygon) in two-dimensional dry foam is independent of bubble size and solely dependent on the number of walls (or edges). The original derivation is based on the rate of gas diffuses through a permeable wall. In our case, the rate of area change of the domain is given by

$$\frac{dA}{dt} = \sum_i \int \mathbf{U}^i \cdot \mathbf{n}^i ds = \int_{\Sigma} \sigma \kappa ds, \quad (34)$$

where  $\mathbf{U}^i \cdot \mathbf{n}^i$  represents the normal velocity of the curve  $i$  per unit length, as discussed earlier. Note that, the above integral of mean curvature is over all

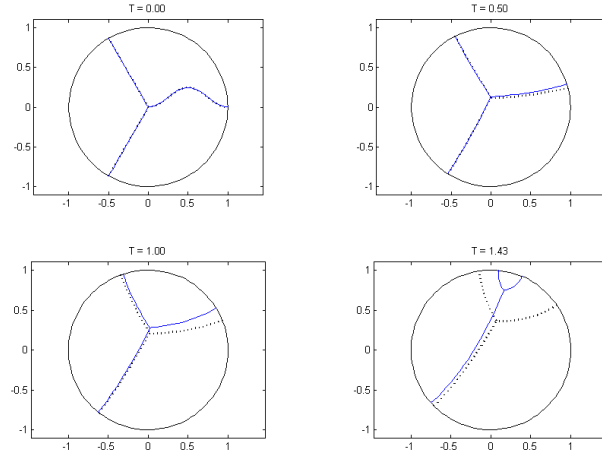


Fig. 3: The time evolution of curve networks: solid lines for  $\beta^i = 0$  and dotted lines for  $\beta^i = 0.25$ .

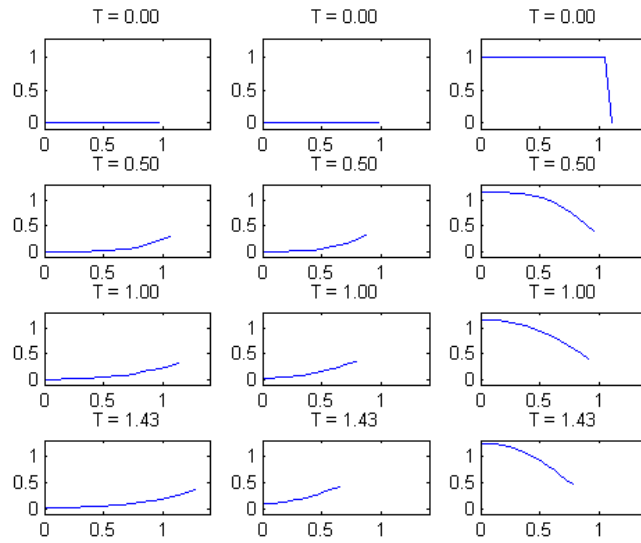


Fig. 4: Distribution of the surfactant concentration on curve 1 (left), curve 2 (center), curve 3 (right).

the curves that enclose the area. When  $\sigma$  is a constant, the enclosed area is polyhedral-shaped with arcs edged, the above integral can be simplified as

$$\frac{dA}{dt} = \sigma \left( \sum_{i=1}^n \alpha_i - 2\pi \right) = \frac{\pi}{3} \sigma (n - 6), \quad (35)$$

where  $\alpha_i = \pi/3$  is the exterior (turning) angle at the vertex, and  $n$  is the number of walls. A similar derivation can be found in [6, 5, 7].

When surface tension varies, however, (35) is no longer valid. For example,  $\alpha_i$  does not always take the value of  $\pi/3$ . It will be interesting to examine how the area changes under a similar setup. We start with a single  $n$ -vertices inner cell with circular arcs and connect those vertices with  $n$  straight lines to the domain boundary. In particular, the cell boundary is a circle of radius 0.5. Note that, the number of lines is the same as the number of vertices on the inner cell. Along each line or circular arc, we lay out a parametrization on those curves. So a cell network with  $n$  vertices should have  $2n$  curves and  $n$  triple-junction.

From the von Neumann law, one can easily see that the cell with more than six walls will grow while the one less than six walls will shrink when the surface tension is constant. More specifically, the area of a cell with  $n = 6$  remains unchanged while the cells with  $n = 5$  and  $n = 7$  should have the same growth (decay) rate. Fig. 5 shows the time evolution of a six vertices cell with (dotted line) or without surfactant (solid line). One can easily see that in the absence of surfactant, the cell area does not change. However, with surfactant, the system behaves differently. For illustrative purposes, we add surfactant only along one line segment  $\Gamma(s, 0) = 1$  initially, and choose  $\beta^1 = 0.75, \beta^2 = 0.5, \beta^3 = 0.25$  in Langmuir equation along the rightmost three curves network (same set up as in Fig. 1) and keep other  $\beta^i = 0.25$ , then the symmetry is broken due to unbalanced surface tension, as shown in Fig. 5. Fig. 6 and Fig. 7 are the corresponding motions for the cells with  $n = 5$  and  $n = 7$ , respectively. It is interesting to see that the unbalanced surface tension slows down the decay rate for the 5 vertices cell area and speeds up the area growth for 7 vertices cell. This is due to the fact with different  $\beta^i$  and surfactant concentration, thus, different surface tension along the rightmost three curves network. Fig. 8 shows the plot of cell area versus time for the cell with and without surfactant for different nodes  $n = 5, 6$ , and 7. One can see the result confirms the prediction by the von Nuemann law when there is no surfactant.

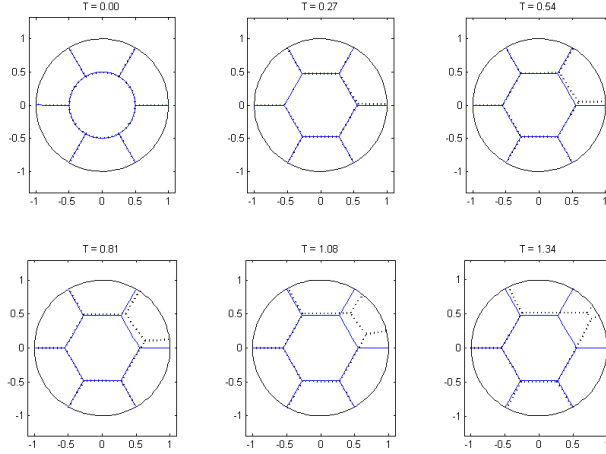


Fig. 5: The time evolution of six nodes cell. Solid line: without surfactant; Dotted line: with surfactant.  $\Gamma^1(s, 0) = \Gamma^2(s, 0) = 0, \Gamma^3(s, 0) = 1$  and the rest of  $\Gamma^i(s, 0) = 0$ ;  $\beta^1 = 0.75, \beta^2 = 0.5, \beta^3 = 0.25$ , the rest of  $\beta^i = 0.25$ .

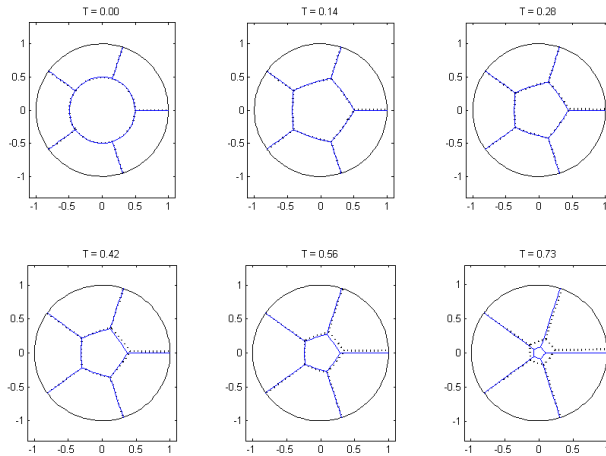


Fig. 6: The time evolution of five nodes cell. Solid line: without surfactant; Dotted line: with surfactant.  $\Gamma^1(s, 0) = \Gamma^2(s, 0) = 0, \Gamma^3(s, 0) = 1$  and the rest of  $\Gamma^i(s, 0) = 0$ ;  $\beta^1 = 0.75, \beta^2 = 0.5, \beta^3 = 0.25$ , the rest of  $\beta^i = 0.25$ .

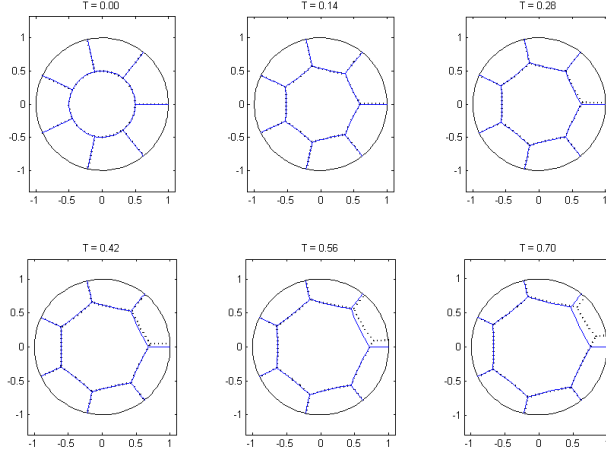


Fig. 7: The time evolution of seven nodes cell. Solid line: without surfactant; Dotted line: with surfactant.  $\Gamma^1(s, 0) = \Gamma^2(s, 0) = 0, \Gamma^3(s, 0) = 1$  and the rest of  $\Gamma^i(s, 0) = 0$ ;  $\beta^1 = 0.75, \beta^2 = 0.5, \beta^3 = 0.25$ , the rest of  $\beta^i = 0.25$ .

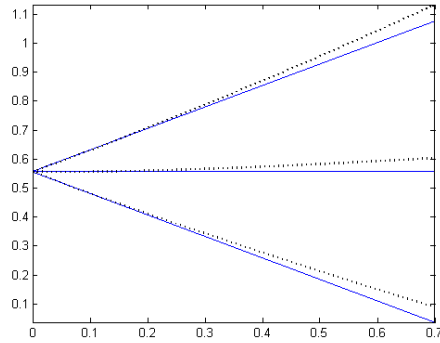


Fig. 8: The cell area versus time, for the cases with and without surfactant. Without surfactant (solid lines), the area evolves as predicted by the von Neumann law while for the case with surfactant (dotted lines), the rate of growth is increased for  $n = 7$  while the rate of decay for  $n = 5$  is decreased. The area for  $n = 6$  also increases.

As our final example, we present the results when surfactant is added initially  $\Gamma^i(s, 0) = 1$  to all the outside line segments connecting the center network (cell) to the boundary. The inner cell boundaries are thus kept clean (without surfactant) initially. In this case, the initial exterior turning angles of the center network are all less than  $\pi/3$ , which reduces the value of  $\sum_{i=1}^7 \alpha_i - 2\pi$  in the von Neumann law. Therefore, we expect that the center network grows much less than the case without surfactant. Furthermore, the cell area should increase again as the surfactant diffuses into the center network, as shown in Figs 9 and 10.

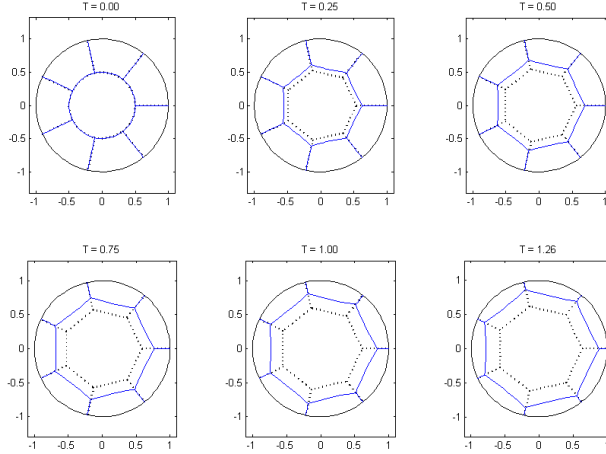


Fig. 9: The time evolution of seven nodes cell. Solid line: without surfactant; Dotted line: with surfactant.  $\beta^i = 0.25$ .

## 4 Conclusion

In this paper, we propose a finite difference method to track curves motion whose normal velocity is determined by surface tension times the local mean curvature. We introduce the surfactant into the curves network and the surface tension varies following surface diffusion of the surfactant. The equations of motion are governed by a parabolic equation for the curve motion as well as a convection-diffusion equation for the surfactant concentration

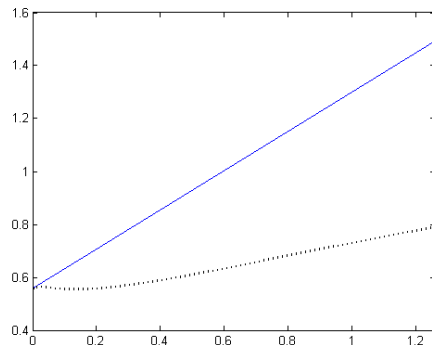


Fig. 10: The cell area versus time, for the cases with and without surfactant for  $n = 7$ . Without surfactant (solid lines), the area evolves as predicted by the von Neumann law while for the case with surfactant (dotted lines), the area decreases in the beginning but increases later on as the surfactant diffuses into the center network.

along each curve. Our numerical method is based on direct discretization of the governing equations and the associated boundary conditions, which conserves the total surfactant mass in the curve network. Numerical examples are presented to illustrate how the inhomogeneous surface tension affects the the motion of the curves and the evolution of the curve network.

## Acknowledgment

M.-C. Lai is supported in part by National Science Council of Taiwan under research grant NSC-97-2628-M-009-007-MY3 and MoE-ATU project. H. Huang is supported by grants from the Natural Science and Engineering Research Council (NSERC) of Canada and the Mathematics of Information Technology and Complex Systems (MITACS) of Canada.

## References

- [1] L. Bronsard, B. T. R. Wetton, A numerical method for tracking curve networks moving with curvature motion, *J. Comput. Phys.*, 120 (1995)

66–87.

- [2] P.G. de Gennes, F. Brochard-Wyart, and D. Quéré, *Capillarity and Wetting Phenomena, Drop, Bubbles, Pearls, Waves*, Springer (2004).
- [3] E. Fried and M.E. Gurtin, A united treatment of evolving interfaces accounting for small deformations and atomic transport: grain-boundaries, phase transitions, epitaxy, *TAM Reports* 1023 (2003), Department of Theoretical and Applied Mechanics, UIUC.
- [4] M.-C. Lai, Y.-H. Tseng, H. Huang, An immersed boundary method for interfacial flows with insoluble surfactant, *J. Comput. Phys.*, 227 (2008) 7279–7293.
- [5] W.W. Mullins, Two-dimensional motion of idealized grain boundaries, *J. Appl. Phys.* 27, (1956) 900–904.
- [6] W.W. Mullins, in *Metal Surfaces: Structure, Energetics, and Kinetics*, W.D.Robertson and N.A.Gjostein, eds.) 17–66 (American Society for Metals, Metals Park, Ohio, 1963).
- [7] von Neumann, J. in *Metal Interfaces* (C.Herring, ed.) 108-110 (American Society for Metals, Cleveland, 1951).
- [8] Z. Pan, B. T. R. Wetton, A numerical method for coupled surface and grain boundary motion, *European J. Appl. Math.* 19 (2008), no 3, 311–327.
- [9] P. Smereka, X. L. G. Russo, and D.J. Srolovitz, Simulation of faceted lm growth in three dimensions: microstructure, morphology and texture, *Acta Materialia* 53 (2005) 1191-1204.
- [10] Y. Pawar, K.J. Stebe, Marangoni effects on drop deformation in an extensional flow: the role of surfactant physical chemistry, I. Insoluble surfactants, *Phys. Fluids* 8 (1996) 1738.
- [11] H. A. Stone, A simple derivation of the time-dependent convective-diffusion equation for surfactant transport along a deforming interface, *Phys. Fluids A* 2(1), (1990) 111–112.

- [12] H. Wong, D. Rumschitzki and C. Maldarelli, On the surfactant mass balance at a deforming fluid interface, *Phys. Fluids*, 8(11) (1996) 3203–3204.